

COMPARISON OF COLLECTOR PERFORMANCE BETWEEN HORIZONTAL AND VERTICAL VACUUM TUBE WATER HEATER

Shi Tianlu^{1,2,3,4}, Li Jinping^{1,2,3,4,*}, Ye Heli^{1,2,3,4}, Huang, Juan Juan^{1,2,3,4}

- (1. Western China Energy & Environment Research Center, Lanzhou University of Technology, Lanzhou 730050, China;
2. Key Laboratory of Complementary Energy System of Biomass and Solar Energy, Gansu Province, Lanzhou 730050, China;
3. China Northwestern Collaborative Innovation Center of Low-carbon Urbanization Technologies, Lanzhou 730050, China;
4. College of Energy and Power Engineering, Lanzhou University of Technology, Lanzhou 730050, China)

ABSTRACT

In order to reveal the difference of collector performance between horizontal and vertical all glass vacuum tube water heaters, the parameters of effective heat collecting area, total solar radiation received by two water heaters under four typical days of the year (spring equinox, summer solstice, autumn equinox and winter solstice) are calculated theoretically. The actual heat collecting performance of the two water heaters is experimentally studied, and the reliability and accuracy of the theoretical analysis are verified. Finally, using FLUENT simulation software to simulate the heat collecting process of two kinds of water heaters. The reason for the difference of collector performance between the two water heaters is explained from the aspect of flow and heat transfer inside the water heater. The results show that only in summer, the collector performance of horizontal tube water heater has advantages. In spring, autumn and winter, the heat collection performance of vertical drain water heater is better.

Keywords: Solar water heater; collector performance; Instantaneous heat collection; Internal convective heat transfer

NONMENCLATURE

θ	the angle between incident light and collector plane
A_e	the effective collector area
A	collector surface area
n	year

\vec{AB}	the normal vector of the collector's open surface
\vec{m}	the angle of incident light
Q_e	the effective heat collection
m_w	the mass of the working water in the water heater
c_p	the specific heat capacity of working water
ΔT	the change of water temperature in the hot water tank during the heat collecting time
A_c	the heat collecting area of the water heater
I	solar radiation
Δt	the duration of the heat collection

1. INTRODUCTION

All glass vacuum tube water heater has great application potential in the field of low temperature heating. Horizontal and vertical tube water heaters are two important types of all glass vacuum tube water heaters. Because of the different installation structures of vacuum tubes, there are some differences in their heat collection performance^[1-3]. At present, there are many studies on all-glass vacuum tube water heater. The collector performance of vacuum tube solar water heater is mainly affected by coating, structure parameters of vacuum tube, physical properties of heat transfer fluid and structure parameters of water heater^[4-6].

In order to improve the collector performance of water heaters, scholars at home and abroad have done a lot of related research around these factors. Solar selective absorption coating is the most important part of solar energy photothermal conversion, which

determines the collector heat collection performance. Selective endothermic coatings with high absorptivity and low emissivity can effectively improve the collector's heat collecting capacity [7]. How to realize the solar selective absorption coating with high solar radiation absorptivity and low infrared radiation emissivity is the core issue of solar thermal utilization research [8,9]. The results show that the absorptivity of solar selective absorbing coatings is generally above 0.95 and the emissivity is below 0.05 [10]. Vacuum tube is the core component of vacuum tube water heater, which has an important impact on the collector performance of the water heater. Yin Zhiqiang [11,12] put forward the relationship between thermal performance parameters of all glass vacuum tubes and vacuum tube structure, coating parameters, ambient temperature and radiation intensity. Badar [13] measured the heat loss of the vacuum interlayer by experimental method. The results show that the heat loss of the vacuum tube is much larger than the expected value. Tang [14] made the average heat loss coefficient experiment of vacuum tube according to the test standard [15]. The results show that the more accurate test results can be obtained only when the ambient temperature changes little. Wu Jiaqing [16] put forward the best vacuum degree of vacuum tube, and gave the method of calculating the service life of vacuum tube. Traditional fluids such as water and air have low heat transfer intensity because of their low thermal conductivity. Searching for new working fluid plays an important role in improving heat transfer intensity of water heater. Xu Jifu [17] found that the heat transfer efficiency of heat conducting oil is much better than that of water by studying the heat collection effect of different working fluids. Compared with traditional heat transfer media, nano-flow has better stability and thermal conductivity [18-22]. The thermal conductivity of nanofluids depends mainly on the shape, size and thermal properties of solid particles [23,24]. Mao Lingbo [25] found that when the carbon-coated copper nanoparticles with a mass fraction of 0.05% were used as the circulating working fluid of the water heater, the heat collection efficiency was obviously improved. The heat transfer performance of the water heater can be effectively optimized by changing the structure of the collector. Jahangiri [26] studied the optimal collector area for different hot water demand, and found that the total thermal gain coefficient of the collector has a significant impact on the performance of the collector. Sivakuma [27] carried out an experimental study on forced convection solar air heater with pin-fin heat absorber. The results

show that the energy efficiency of the forced convection solar air heater with pin-fin heat absorber is 3%-12% higher than that of the flat heat absorber, and the collector performance has been significantly improved. Heydari et al. [28] studied the influence of spiral grooves on the performance of solar water heaters from both experimental and numerical aspects. The results show that the average thermal efficiency of spiral groove dual-channel solar air heater is 14.7% higher than that of single-channel solar air heater and 8.6% higher than that of dual-channel fin solar air heater with the same mass flow rate.

However, there is no comparative study on the difference of all-day heat collection performance between horizontal and vertical drainage glass vacuum tube water heaters under forced circulation. There is always a controversy about which water heater has better heat collection performance. Therefore, it is necessary to conduct a comprehensive and in-depth study on the collector performance of the two water heaters.

2. TEST METHOD AND CALCULATION BASIS

2.1 Test method

According to the national standard [29], the horizontal and vertical all-glass vacuum collector solar hot water system was constructed in Lanzhou City (north latitude 36°03', east longitude 103°40'). As shown in Figure 1, the thickened line part represents the forced circulation pipeline. Both water heaters consist of 30 all glass vacuum tubes. The specification of all glass vacuum tubes is $\Phi 58 \times 1800$ mm. The water heater is positioned to the south, and the angle between the collector plane and the horizontal plane is 45 degrees.

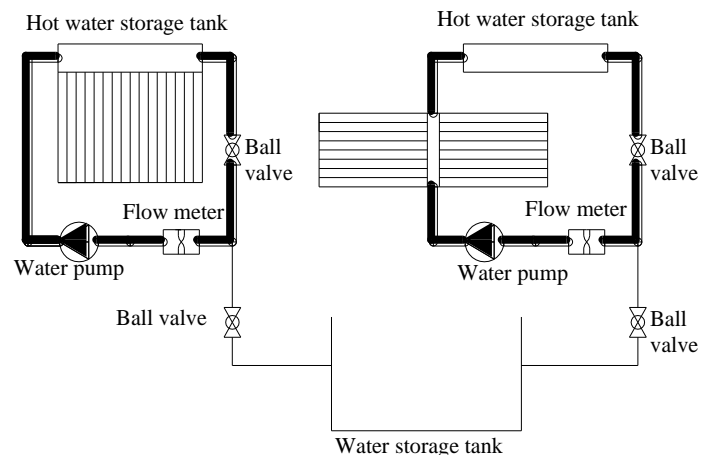


Fig.1 All-glass evacuated tubular solar water heating system

The parameters of the measuring equipment are detailed in Table 1.

Table 1 Experimental Instruments

Device name	Specifications	Vendor
Hot film wind speed sensor	Model: YGC-RMFS,	Guangzhou Xizheng Automation Technology Co., Ltd.
	Range: 0~5 m, Precision: ±0.2% FS	
Solar radiation tester	Model: TBS-2-2,	Jinzhou Huayi IOT Measurement and Control Technology Co., Ltd.
	Range:0.3~3 μm, Precision: 2%, Sensitivity: 7~14 μV/W·m ²	
Flow meter	Model: LWGY-32A,	Shanghai Fan Yang Electrical Co., Ltd.
	Output: 1-5 V, Range: 0-5 m ³ /h, Precision: 0.5%	
Temperature Sensor	Model: Pt100	Beijing West Air China Technology Co., Ltd.
	Range: -50~150 °C, Precision: 0.1 °C	
Data acquisition instrument	Model: Agilent3493A,	Shenzhen Hongxinyu Instrument Co., Ltd.
	Scanning frequency: 250 channel/s	

Before the start of the test, the water in the water heater is first emptied, and then 320 L of water at the same temperature is added. Open the circulating pump before the test begins. Regulate the valve and adjust the flow rate to 800 L/h. The circulating pump runs continuously until the end of the test. In addition, the surface of the vacuum tube is wiped clean to avoid the influence of surface dust on the test results. The test data were collected by Agilent 34970A data acquisition instrument. The acquisition interval was 2 seconds. The measurement parameters include the temperature of hot water storage tank, ambient temperature, solar radiation, wind speed, water flow of circulating pipeline, etc. The test time ranged from 06:00 to 20:00.

2.2 Calculation basis

According to the literature^[30], the solar altitude angle and azimuth angle can be calculated. According to the altitude and azimuth of solar radiation, the angle θ between incident light and collector plane can be further calculated by using space vector knowledge. The effective collector area A_e can be calculated from the angle and collector surface area A . The instantaneous solar radiation received by the water heater Q_i can be calculated from the

effective collector area A_e and the corresponding solar radiation I . The calculation formula is as follows.

$$\theta = \arcsin \frac{|\overline{AB} \cdot \overline{m}}{|\overline{AB}| |\overline{m}|} \quad (2.1)$$

$$A_e = A \cos \theta \quad (2.2)$$

$$Q_i = I \times A_e \quad (2.3)$$

The effective heat collection Q_e is the actual heat collection of the hot water tank, which can be calculated by formula (1):

$$Q_e = m_w c_p \Delta T \quad (2.4)$$

The average effective heat collection efficiency η is the ratio of the effective heat collection amount to the total solar radiation amount during the heat collection time, which can be calculated by the formula (2):

$$\eta = \frac{Q_e}{A_c I \Delta t} = \frac{m_w c_p \Delta T}{A_c I \Delta t} \times 100\% \quad (2.5)$$

3. RESULTS AND ANALYSIS

3.1 Theoretical calculation and analysis

The calculation results of the effective collector area are shown in the figure 3.1, 3.2, 3.3 and 3.4. Comparing with figs. 3.1, 3.2, 3.3 and 3.4, it can be found that the effective heat collecting area of horizontal tube water heater is significantly higher than that of vertical tube water heater in most collecting time around the summer solstice. However, in the spring equinox, autumn equinox and winter solstice, the effective heat collecting area of the horizontal pipe water heater is larger than that of the vertical pipe water heater only at about 13:10 noon. In other collecting time, the effective heat collecting area of the vertical pipe water heater is obviously larger than that of the horizontal pipe water heater.

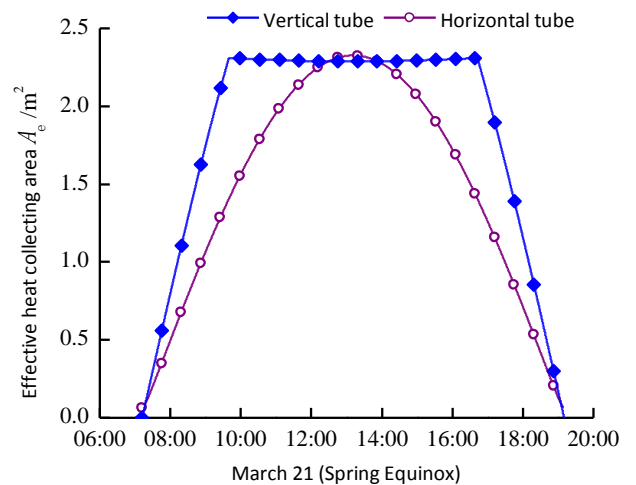


Fig.3.1 Effective heat collecting area of water heater at vernal equinox

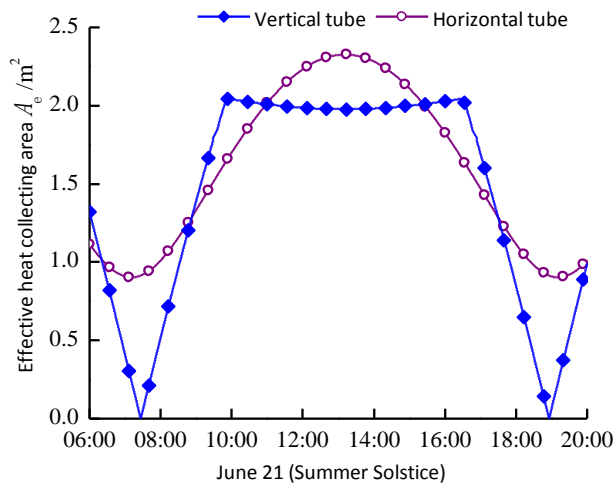


Fig.3.2 Effective heat collecting area of water heater at summer solstice

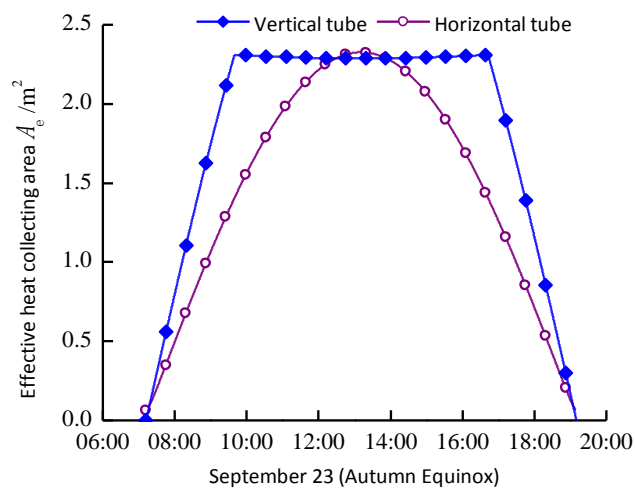


Fig.3.3 Effective heat collecting area of water heater at autumn equinox

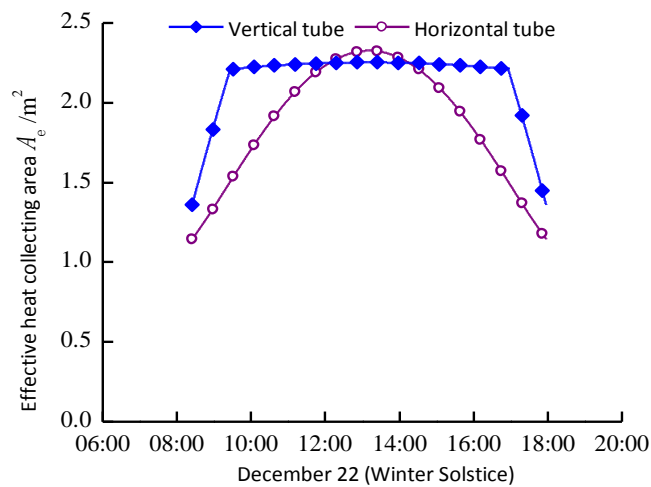


Fig.3.4 Effective heat collecting area of water heater at winter solstice

In addition, for vertical pipe water heaters, the shelter time between tubes is up to 8 hours in summer solstice, 3 hours in winter solstice, and 5 hours in spring and autumn equinoxes. For horizontal pipe water heaters, there is no shielding between tubes.

The total solar radiation received in four typical days is shown in Figure 3.5. As can be seen from Fig. 3.5, the highest total solar radiation receiving time for horizontal water heaters is the summer solstice, which is 61.8 MJ. The minimum time to receive total solar radiation is the winter solstice, which is only 48.8 MJ. For vertical drain water heaters, the highest total solar radiation received during the whole day is the vernal equinox, which is 70.1 MJ. The autumn equinox was slightly lower than the spring equinox (65.5 MJ), followed by the summer solstice (57.1 MJ). The lowest is the winter solstice, which is only 53.8 MJ. It can be seen that the total solar radiation received by the horizontal tube water heater is higher than that of the vertical tube water heater only at the summer solstice, and the total solar radiation received by the vertical tube water heater during the spring equinox, autumn equinox and winter solstice is significantly higher than that of the horizontal tube water heater.

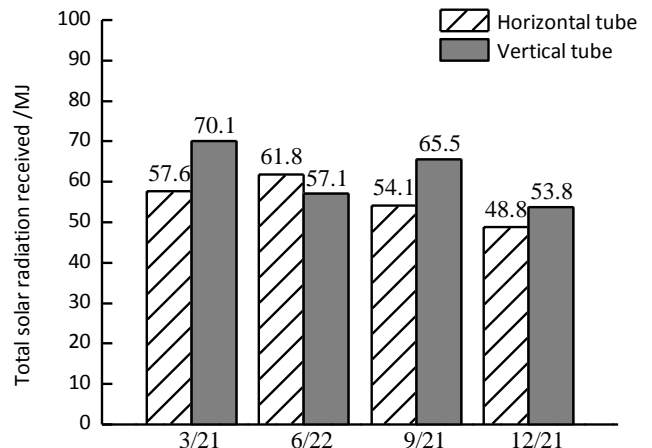


Fig.3.5 The total solar radiation received in four typical days

3.2 Experimental results and analysis

The experimental data for the whole year are shown in table 3.1, 3.2, 3.3 and 3.4. Comparing with tables table 3.1, 3.2, 3.3 and 3.4, it can be seen that the average effective heat collection efficiency of horizontal tube water heater is higher than that of vertical tube water heater only in the period around the summer solstice in June. In the period of spring equinox, autumn equinox and winter solstice, the effective heat collection efficiency and average effective heat collection efficiency of vertical pipe water heater are higher than that of horizontal pipe water heater. The

experimental results are consistent with the theoretical results, which shows that the theoretical calculation is accurate and reliable.

Table 3.1 Result of experimental data in March

Experimental Time	Structure	Effective Heat Collection/MJ	Average Effective Heat Collection Efficiency
March 21	Horizontal	33.3	58.8%
	Vertical	35.5	62.7%
March 22	Horizontal	27.2	59.3%
	Vertical	28.1	61.2%
March 23	Horizontal	26.9	60.8%
	Vertical	28.2	63.7%
March 24	Horizontal	33.5	55.9%
	Vertical	36.9	61.6%
March 25	Horizontal	28.3	57.8%
	Vertical	31.2	63.8%

Table 3.2 Result of experimental data in June

Experimental Time	Structure	Effective Heat Collection/MJ	Average Effective Heat Collection Efficiency
June 21	Horizontal	39.4	71.3%
	Vertical	34.2	61.9%
June 22	Horizontal	31.5	65.0%
	Vertical	28.8	59.4%
June 23	Horizontal	35.6	72.8%
	Vertical	30.8	62.9%
June 24	Horizontal	31.8	70.7%
	Vertical	28.7	63.8%
June 25	Horizontal	38.3	71.2%
	Vertical	33.5	62.2%

Table 3.3 Result of experimental data in September

Experimental Time	Structure	Effective Heat Collection/MJ	Average Effective Heat Collection Efficiency
September 21	Horizontal	29.5	60.9%
	Vertical	32.2	66.4%
September 22	Horizontal	30.8	63.9%
	Vertical	32.5	67.4%
September 23	Horizontal	29.7	62.5%
	Vertical	31.6	66.5%
September 24	Horizontal	31.3	61.9%
	Vertical	32.8	64.9%
September 25	Horizontal	31.2	63.8%
	Vertical	32.9	67.2%

Table 3.4 Results of experimental data for December

Experimental Time	Structure	Effective Heat Collection/MJ	Average Effective Heat Collection Efficiency
December 20	Horizontal	18.4	30.9%
	Vertical	20.1	33.8%
December 21	Horizontal	17.8	30.4%
	Vertical	20.2	34.5%
December 22	Horizontal	18.7	31.1%
	Vertical	21.0	34.8%
December 23	Horizontal	19.6	31.6%
	Vertical	22.3	35.9%
December 24	Horizontal	18.9	31.7%
	Vertical	21.3	35.6%

3.3 Simulation results and analysis-

The whole-day heat collection process of water heater was simulated by FLUENT simulation software. Two time points (8:00 and 13:00) were selected to analyze the flow inside the vacuum tube. At 8:00, the solar radiation intensity is 448.1 W/m², and at 13:00, the solar radiation intensity is 987.2 W/m².

For the convenience of analysis, the vacuum tube is divided into four parts: front part, In the middle and front part, mid-posterior part and tail part, as shown in Figure 3.6.

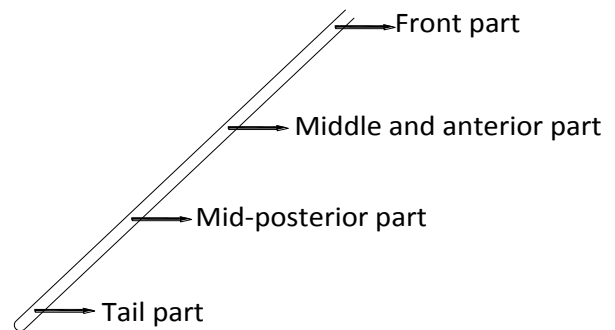
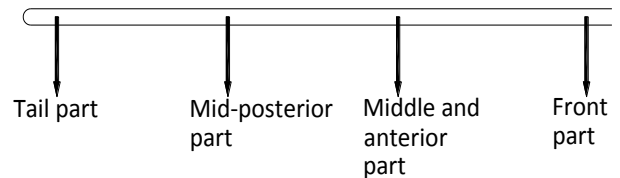


Fig.3.6 Schematic diagram of vacuum tube location

At 8:00, the solar radiation is 448.1 W/m². The internal fluid motion vectors of the front part, In the middle and front part, mid-posterior part and tail part of the horizontal tube are shown in Fig. 3.7, 3.8, 3.9 and 3.10,

respectively. The unit of fluid flow velocity is m/s.

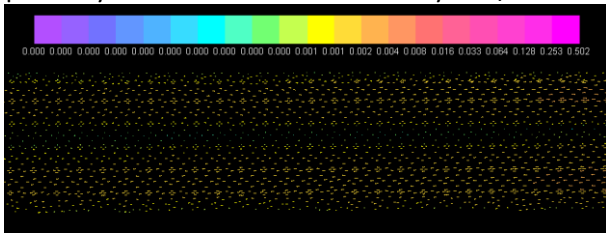


Fig.3.7 Vector diagram of fluid motion at front part of horizontal pipe at 8:00

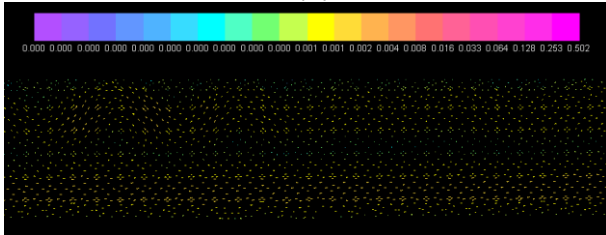


Fig.3.8 Vector diagram of fluid at the middle and front part of horizontal pipe at 8:00

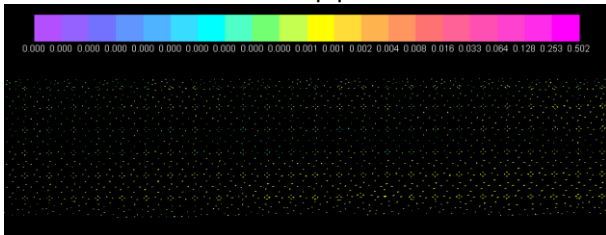


Fig.3.9 Fluid motion vector diagram at mid-posterior part of horizontal pipe at 8:00

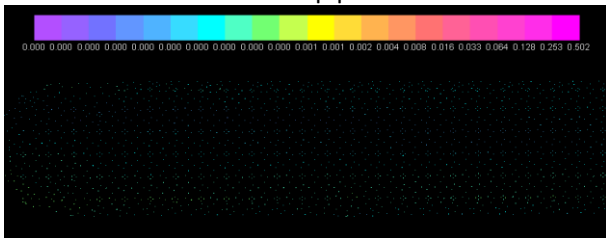


Fig.3.10 Vector diagram of fluid motion at the tail part of horizontal pipe at 8:00

From figs.3.7, 3.8, 3.9 and 3.10, it can be seen that when the solar radiation is 448.1 W/m^2 , there are some stratification phenomena in the front part and the middle and front part of the transverse row vacuum tube. The upper layer of hot fluid flows out of the tube and the lower layer of cold fluid flows into the tube, but the flow speed is relatively slow. The stratification of the fluid in the middle and rear parts of the vacuum tube is not obvious, and the flow velocity of the fluid slows down obviously. There is no stratification at the tail end, and the fluid is basically not flowing.

At 13:00, the solar radiation is 987.2 W/m^2 . The internal fluid motion vectors of the front part, In the middle and front part, mid-posterior part and tail part of the

horizontal tube are shown in figs. 3.11, 3.12, 3.13 and 3.14, respectively.

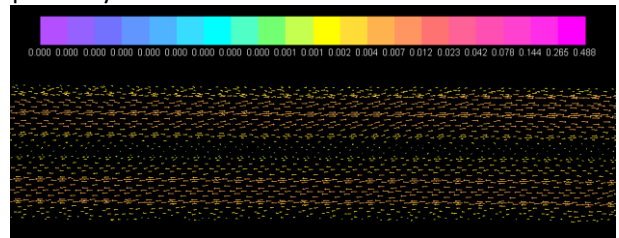


Fig.3.11 Vector diagram of fluid motion at front part of horizontal pipe at 13:00

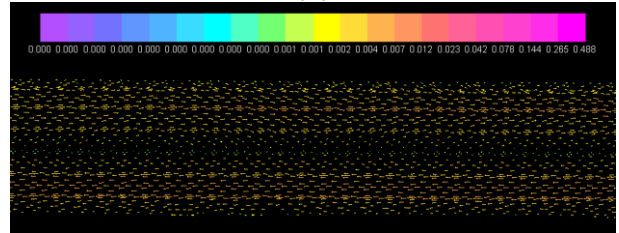


Fig.3.12 Vector diagram of fluid at the middle and front part of horizontal pipe at 13:00

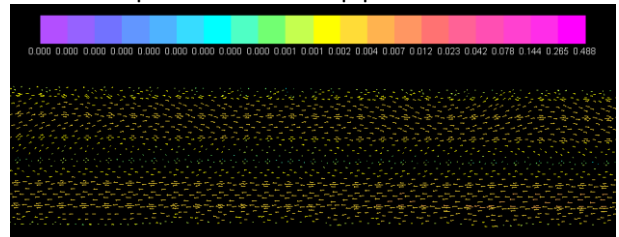


Fig.3.13 Fluid motion vector diagram at mid-posterior part of horizontal pipe at 13:00

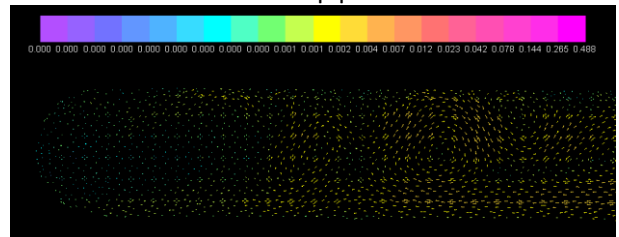


Fig.3.14 Vector diagram of fluid motion at the tail part of horizontal pipe at 13:00

From figs. 3.11, 3.12, 3.13, and 3.14, it can be seen that when the solar radiation is 987.2 W/m^2 , the stratification of fluid in front part, In the middle and front part and mid-posterior part of the transverse vacuum tube is very good, the fluid flow speed is faster, and it can effectively exchange heat with the outside. Only in the tail part, there are vortices, the fluid flow is slow, and the exchange speed of heat with the outside is slow. Compared with the solar radiation of 448.1 W/m^2 , the flow state of the inner fluid in the transverse row tube has been significantly improved, and the inner fluid can effectively exchange cold and hot fluids with the outer fluid.

At 8:00, the solar radiation is 448.1 W/m^2 . The internal fluid motion vectors of the front part, In the middle and

front part, mid-posterior part and tail part of the vertical tube are shown in Fig. 3.15, 3.16, 3.17 and 3.18, respectively. The unit of fluid flow velocity is m/s.

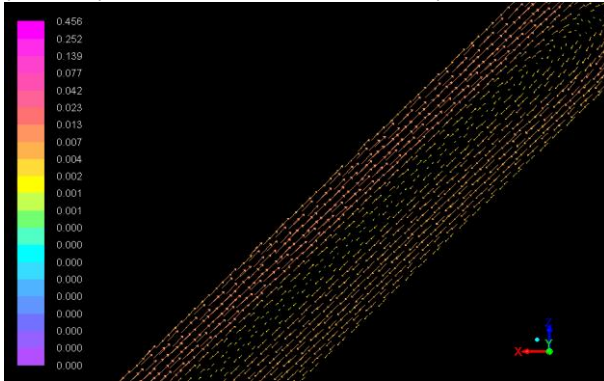


Fig.3.15 Vector diagram of fluid motion at front part of vertical pipe at 8:00

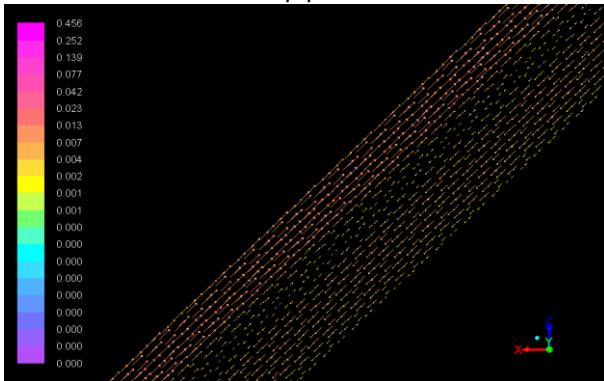


Fig.3.16 Vector diagram of fluid at the middle and front part of vertical pipe at 8:00

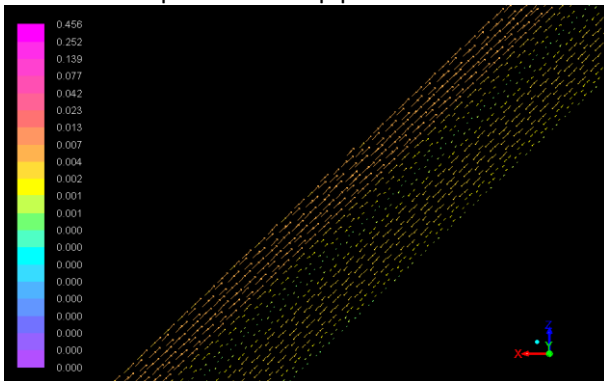


Fig.3.17 Fluid motion vector diagram at mid-posterior part of vertical pipe at 8:00

From figs. 3.15, 3.16, 3.17 and 3.18, it can be seen that when the solar radiation is 448.1 W/m^2 , the stratification of the fluid in the front part, In the middle and front part and mid-posterior part of the vertical vacuum tube is better, the flow and heat transfer of the cold and hot fluids are good, and the flow velocity of the fluid in the tail part is slowed down, but there are stratification phenomena, and the fluid has a certain flow velocity.

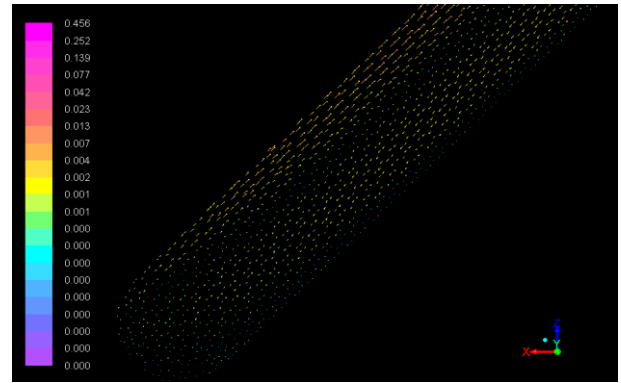


Fig.3.18 Vector diagram of fluid motion at the tail part of vertical pipe at 8:00

At 13:00, the solar radiation is 987.2 W/m^2 . The internal fluid motion vectors of the front part, In the middle and front part, mid-posterior part and tail part of the vertical tube are shown in figs. 3.19, 3.20, 3.21 and 3.22, respectively.

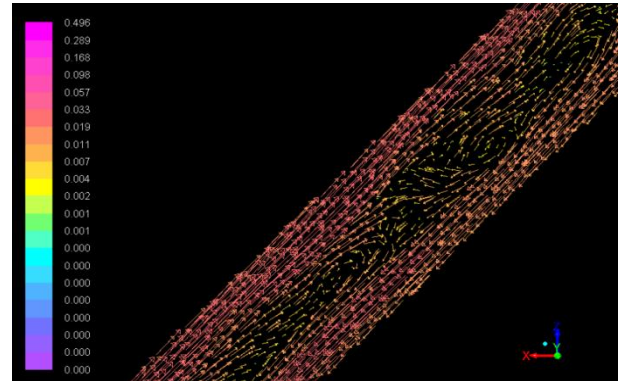


Fig.3.19 Vector diagram of fluid motion at front part of vertical pipe at 13:00

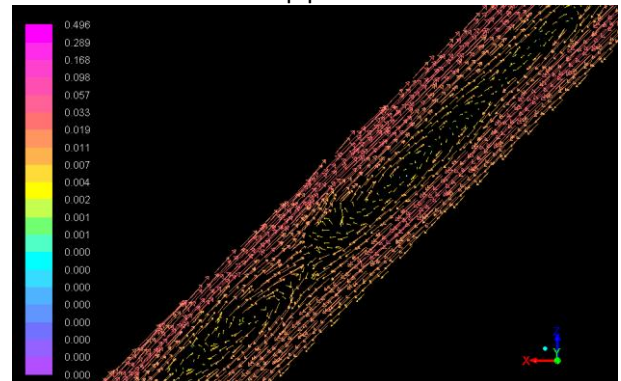


Fig.3.20 Vector diagram of fluid at the middle and front part of vertical pipe at 13:00

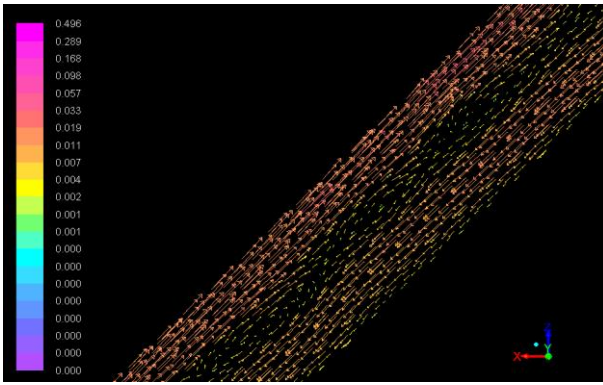


Fig.3.21 Fluid motion vector diagram at mid-posterior part of vertical pipe at 13:00

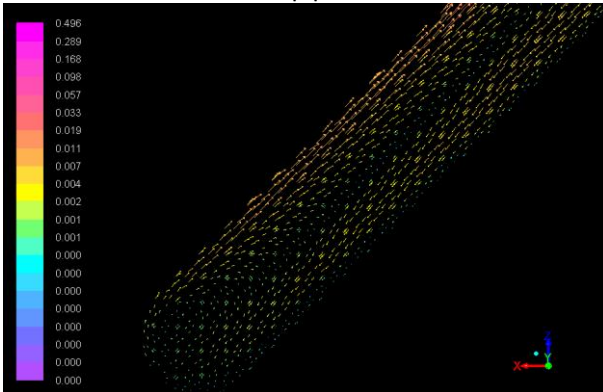


Fig.3.22 Vector diagram of fluid motion at the tail part of vertical pipe at 13:00

It can be seen from figs. 3.19, 3.20, 3.21 and 3.22, when the solar radiation is 987.2 W/m^2 , stratification occurs at the front, front, rear and tail of the vertical vacuum tube, but there are many small vortices at the front part and the middle and front part of the vacuum tube. The appearance of vortices makes some of the upper hot fluids return to the vacuum tube with the cold fluids before they flow out of the vacuum tube. At the same time, some of the cold fluids flow out with the hot fluids before they enter the lower part of the vacuum tube, resulting in poor heat exchange between the vacuum tube and the outside. Compared with the solar radiation of 448.1 W/m^2 , the fluid flow velocity inside the vacuum tube has been improved, but the swirl phenomenon restrains the exchange speed between the vacuum tube and the external heat.

4. CONCLUSIONS

(1) In terms of effective heat-collecting area, at the summer solstice, the effective heat-collecting area of horizontal tube water heater is significantly higher than that of vertical tube water heater during most of the day's heat-collecting time. In the spring equinox, autumn equinox and winter solstice, the effective heat collecting area of the horizontal tube water heater is larger than that of the vertical tube water heater only in a short period around 13:10 noon. In most other collecting time, the effective heat

collecting area of the vertical tube water heater is obviously larger than that of the horizontal tube water heater.

(2) In terms of the total solar radiation received by water heaters throughout the day, only in the summer solstice, the total solar radiation received by horizontal tube water heaters is higher than that of vertical tube water heaters. In the spring equinox, autumn equinox and winter solstice, the total solar radiation received by vertical tube water heaters throughout the day is significantly higher than that of horizontal pipe water heaters.

(3) When the solar radiation is low, there is no good stratification of fluid motion in the transverse vacuum tube, and the heat transfer with the external water tank is slow. A good fluid moving layer has been formed inside the vertical vacuum tube, which can exchange heat efficiently with the external water tank. The collector performance of vertical water heater is better than that of horizontal water heater.

(4) When the solar radiation is strong, the velocity of fluid movement in the vacuum tube of the transverse water heater is accelerated, forming a good motion stratification without obvious vortices, which can effectively exchange heat with the external water tank. The velocity of fluid movement in the vacuum tube of vertical water heater increases obviously, but there are many vortices. The appearance of vortices destroys the fluid moving layer and hinders the heat exchange between the vacuum tube and the external water tank, which results in the lower collector performance of the vertical water heater than that of the horizontal water heater.

ACKNOWLEDGEMENT

This work was supported by National Key Research and Development Program Project (2018YFB0905104), National Natural Science Foundation Project (51676094), Organization Department of Gansu Provincial Party Committee of the Communist Party of China "Longyuan Youth Innovation Talents Support" Project (Innovation Team, Gan Group Tongzi [2014] 93), Gansu University Collaborative Innovation Technology Team Project, Gansu Province International Science and Technology Cooperation Project Project (1604WKCA009), Lanzhou Talent Innovation and Entrepreneurship Project (2017-RC-34), Gansu Natural Science Foundation (1508RJA051) and Lanzhou University of Technology Hongliu First-class Discipline Fund.

REFERENCE

- [1] Yan Suying, Huang Haiyan, Tian Rui, etc. Mechanism analysis for heat transfer enhancement with all glass vacuum solar water heater[J]. *Journal of Engineering Thermophysics*, 2012; 33(3):485-488.
- [2] Hossain M S, Saidur R, Fayaz H, et al. Review on solar waterheater collector and thermal energy performance of circulating pipe[J]. *Renew able and Sustainable Energy Review s*, 2011; 15(8):3801-3812.
- [3] Zhao Haiou, Li Xuguang, Zhao Juan, et al. Experimental study on thermal performance of solar water heaters with different inclinations in Beijing area [J]. *Solar Energy*, 2013; 24: 54-56.
- [4] Yan Suying, Huang Haiyan, Tian Rui, etc. Mechanism analysis for heat transfer enhancement with all glass vacuum solar water heater[J]. *Journal of Engineering Thermophysics*, 2012, 33(3):485-488.
- [5] Hossain M S, Saidur R, Fayaz H, et al. Review on solar waterheater collector and thermal energy performance of circulating pipe[J]. *Renew able and Sustainable Energy Review s*, 2011, 15(8):3801-3812.
- [6] Zhao Haiou, Li Xuguang, Zhao Juan, et al. Experimental study on thermal performance of solar water heaters with different inclinations in Beijing area [J]. *Solar Energy*, 2013 (24): 54-56.
- [7] Ma Pengjun, Geng Qingfen, Liu Gang. Rent investigations in solar spectroscopy [J]. *Material report*, 2015, 29 (1): 48-53.
- [8] Selvakumar N, Barshilia H C. Review of physical vapor deposited (PVD) spectrally selective coatings for mid-and high-temperature solar thermal applications[J]. *Solar Energy Materials and Solar Cells*, 2012, 98:1-23.
- [9] Zhang Lin, Zhao Teng, Chen Dapeng, et al. Research progress and prospect of solar selective absorption film [J]. *Vacuum*, 2013, 50 (3): 57-6.
- [10] Wang Cong, Daibei, Yu Jiayu, et al. Rescent development and advance of solar photoelectric materials and photothermal conversion materials [J]. *journal of the chinese ceramic society*, 2017, 11:1555-1567.
- [11] Yin Zhiqiang, Tang Xuan. Solar thermal performance of all — glass evacuated collector tubes[J]. *Acta Energiae Solaris Sinica*, 2001, 22 (1): 1—5.
- [12] Yin Zhiqiang, Yan Xiyuan, Chen Tenghua, et al. The thermal performance of evacuated collector tubes with solar absorbing coatings [J]. *Acta Energiae Solaris Sinica*, 1996(1): 50—56.
- [13] Abdul Waheed Badar, Reiner Buchholz, Felix Ziegler. Experimental and theoretical evaluation of the overall heat loss coecient of vacuum tubes of a solar collector[J]. *Solar Energy*, 2011, 85(7):1447-1456.
- [14] Runsheng Tang, Yuqin Yang, Wenfeng Gao. Comparative studies on thermal performance of water-in-glass evacuated tube solar water heaters with different collector tilt-angles[J]. *Solar Energy*, 2011, 85(7):1381-1389.
- [15] GB/T17049-2005, all glass vacuum solar collector [S].
- [16] Wu Jiaqing, Tao Zuyan, Wang Fengchun, et al. Vacuum acquisition and vacuum life of glass vacuum collector tubes [J]. *Journal of Tsinghua University*, 1982, 22 (2): 89-98.
- [17] Xu Jifu, Zhu Yuezhao, Jiang Jinzhu, et al. Temperature field and flow field analysis of solar vacuum tube heat pipe collector [J]. *Fluid Machinery*, 2009, 37 (2): 61-64.
- [18] Zhou Lu, Ma Hong He, Ma Suxia, et al. [J]. Review of the preparation technology of nano-copper for solar collectors and the properties of copper nanofluids [J]. *Material report*, 2018, 32 (15): 2576-2583.
- [19] Zhao Xudong. Application of nanofluids to enhance heat transfer in gas turbine intercoolers [D]. Beijing: China Ship Research Institute, 2012.
- [20] Li Qiang, Xuan Yimin, Jiang Jun, et al. Experimental investigation on flow and heat transfer feature of a nanofluids for aerospace thermal management[J]. *Journal of Astronautics*, 2005, 26 (04): 391-394.
- [21] Quwei, Yuan Dazhong, Li Yuhua. Flow and heat transfer performance in nano-flow pulsating heat pipes [J]. *Journal of Engineering Thermophysics*, 2009, 30 (10): 1697-1699.
- [22] Ni Yu. Study on Natural Circulation Solar Energy Collection System with Nanofluids as Working Fluids [D]. Hangzhou: Zhejiang University, 2011.
- [23] Eastman J A , Choi S U S , Li S , et al. Anomalously increased effective thermal conductivities of ethylene glycol-based nanofluids containing copper nanoparticles[J]. *Applied Physics Letters*, 2001, 78(6):718-720.
- [24] Yimin Xuan, Qiang Li, Heat transfer enhancement of nanofluid[J]. *International Journal of Heat and Fluid Flow*, 2000, 21:58—64.
- [25] Mao Lingbo, Zhang Renyuan, Ke Xiufang, et al. Photo-thermal properties of nanofluid-based solar collectors [J]. *Acta Energiae Solaris Sinica*, 2009, 30 (12): 1647-1652.

- [26] Jahangiri Mamouri S, Bénard, André. New design approach and implementation of solar water heaters: A case study in Michigan[J]. Solar Energy, 2018, 162: 165-177.
- [27] Sivakumar S, Siva K, Mohanraj M. Experimental thermodynamic analysis of a forced convection solar air heater using absorber plate with pin-fins[J]. Journal of Thermal Analysis and Calorimetry, 2019(15).
- [28] Heydari A, Mesgarpour M. Experimental analysis and numerical modeling of solar air heater with helical flow path[J]. Solar Energy, 2018, 162:278-288.
- [29] GB/T 18708 — 2002, Test methods for thermal performance of domestic solar water heating systems [S]
- [30] Wang Hui, Cui Lianyan. Calculating algorithm of solar altitude angle and azimuth angle [J]. Electronic technology and software engineering, 2015; 17: 167-167.